# Eco-VTF

## Fuel-efficient vessel train formations for all-electric autonomous ships

Chen, Linying; Haseltalab, Ali; Garofano, Vittorio; Negenborn, Rudy R.

**DOI**
10.23919/ECC.2019.8796033

**Publication date**
2019

**Document Version**
Accepted author manuscript

**Published in**
Proceedings of the 18th European Control Conference (ECC 2019)

# Eco-VTF: Fuel-Efficient Vessel Train Formations for All-Electric Autonomous Ships

Linying Chen, Ali Haseltalab, Vittorio Garofano and Rudy R. Negenborn

***Abstract*— In this paper, a distributed control approach is proposed to enable fuel-efficient Vessel Train Formations (VTF) in inland waterways and port areas for addressing the efficiency and environmental issues of transport over water. For path tracking, collision avoidance, and consensus over the VTF speed a distributed Model Predictive Control (MPC) algorithm is adopted which uses the Alternating Direction Method of Multipliers (ADMM) to guarantee path following and consensus between vessels. The all-electric Direct Current (DC) configuration is considered for the Power and Propulsion Systems (PPS) of the autonomous vessels under study. Considering their PPS specification, the vessels negotiate with each other to agree on the most efficient speed for all the vessels in the VTF. Simulation results suggest that a significant amount of fuel saving can be obtained by using the proposed approach.**

## I. Introduction

Autonomous shipping has been studied extensively in academia and industry in the last few years. It is believed that the adoption of autonomous ships for different transport purposes can lead to significant benefits ranging from capital cost to safety issues. There has been a significant investment by the states and industry to enable autonomous shipping for inland and seagoing vessels. However, there are numerous challenges on the way of having a fully autonomous ship, such as maneuvering control, interaction management with the surrounding environment, efficiency and fault-detection and isolation issues [1], [2], [3].

The problem of maneuvering and trajectory tracking control has been studied more than the others by the scientific community as several approaches have been introduced to increase the robustness and decrease the error of trajectory tracking in the presence of environmental disturbances. Adaptive schemes are introduced in [4], [5], [6] where uncertainty within the model and environmental disturbances are handled using neural networks, fuzzy logic and model reconfiguration. The adoption of model-based approaches such as Model Predictive Control (MPC) algorithms are investigated in [7], [8] where the results suggest a remarkable decrease in the trajectory following error.

Increasing the fuel efficiency of vessels is a critical issue in the domain of transport over water. Several international organizations and authorities, including International Maritime Organization (IMO), are imposing different constraints on $CO_2$ and $NO_x$ emissions produced by vessels to decrease the adverse ecological effects of inland and seagoing transport. The problem of fuel consumption and efficiency is being addressed from several perspectives ranging from designing efficient power and propulsion systems [2], [9] to fuel-efficient on-board energy management approaches [1], [10], [11]. One of the futuristic and favorable power and propulsion configurations is the all-electric Direct Current (DC) configuration where the loads are fed through a DC grid. Among several advantages of DC power and propulsion systems optimal engine loading, variable diesel engine speed and fuel efficiency can be numerated which makes it suitable for ships with different operational profiles [2], [12].

Recently, researchers have started investigating the possibility and efficiency of moving the autonomous vessels in formation, inspired by similar works in robotics and vehicular technology domains. In [13], the problem of collision avoidance is addressed using distributed model predictive control techniques. A robust distributed control technique is adopted in [14] so that individual vessels can handle additive disturbances and avoid collision. Enabling the Vessel Train Formation (VTF) of vessels is investigated in [15] where a distributed control scheme is used for simultaneous grouping and collision avoidance of vehicles.

To the best of our knowledge, for the first time in the literature, the problems of trajectory tracking, cooperative control of autonomous vessels and fuel efficiency are brought together in this paper where the objective is to enable fuel efficient VTF to not only address the ever increasing cargo capacity demands in inland waterways and port areas but also to tackle the fuel consumption and emissions problems. In this regard, after presenting a dynamical maneuvering model for an individual vessel and representing the futuristic all-electric DC power and propulsion systems, a cooperative approach is proposed to enable Ecological Vessel Train Formation (Eco-VTF). The approach is based on distributed MPC which guarantees trajectory tracking and consensus over VTF velocity between multiple vessels. In this framework, the vessels negotiate over the speed of the VTF by considering their efficient area in the Specific Fuel Consumption (SFC) curve of their diesel engine and maximum deliverable power by the on-board energy storage that is charged on-shore. The Alternating Direction Method of Multipliers (ADMM) is adopted for solving the consensus problem iteratively. The simulation results indicate that a significant amount of fuel saving can be achieved if the proposed Eco-VTF approach is adopted.

The remainder of this paper is organized as follows. In Section 2, the ship maneuvering model and the on-board power and propulsion system are discussed. In Section 3, the Eco-VTF approach is formulated and presented. The

The authors are with the Department of Maritime and Transport Technology, Delft University of Technology, Delft, The Netherlands. Email: {L.Chen-2, A.Haseltalab, V.Garofano, R.R.Negenborn}@tudelft.nl.

simulation experiment results are presented in Section 4. In Section 5, concluding remarks are given and the future research directions are discussed.

## II. Dynamic model

### A. 3 DOF dynamic model of an ASV

In this paper, we consider $n$ heterogeneous Autonomous Surface Vessels (ASVs). Their dynamics are described with the 3 DOF model proposed in [16], with varying parameter values:

$$\dot{\eta}_i = R(\psi_i)\nu_i \tag{1}$$

$$M_i\dot{\nu}_i = -C_i(\nu_i)\nu_i - D_i\nu_i + \tau_i, \tag{2}$$

where $R(\psi_i)$ is a rotation matrix,

$$R(\psi_i) = \begin{bmatrix} \cos(\psi_i) & -\sin(\psi_i) & 0 \\ \sin(\psi_i) & \cos(\psi_i) & 0 \\ 0 & 0 & 1 \end{bmatrix},$$

$\eta_i = [x_i, y_i, \psi_i]^{\mathrm{T}}$ are coordinates $x_i$, $y_i$, and heading angle $\psi_i$ in the North-East-Down coordinate system; $\nu_i = [u_i, v_i, r_i]^{\mathrm{T}}$ are surge and sway velocities $u_i$, $v_i$, and yaw rate $r_i$ in Body-fixed reference frame; $\tau_i = [\tau_{u_i}, \tau_{v_i}, \tau_{r_i}]^{\mathrm{T}}$ are forces $\tau_{u_i}$, $\tau_{v_i}$, and moment $\tau_{r_i}$ in Body-fixed reference frame. $M_i$ is the system inertia matrix, including rigid-body and added mass matrices, $C_i$ is the Coriolis-centripetal matrix, including rigid-body and added mass Coriolis-centripetal matrices, $D_i$ is the damping force. In this paper, we consider a linear damping force.

With $x_i = \begin{bmatrix} {\eta_i}^{\mathrm{T}} & {\nu_i}^{\mathrm{T}} \end{bmatrix}^{\mathrm{T}}$ and $\tau_i$ the system state and input, respectively, the dynamic model (1)-(2) can be expressed as

$$\begin{aligned} \dot{x}_i &= f_i(x_i, \tau_i) \\ &= \begin{bmatrix} \mathbf{0}^{3\times3} & R_i(\psi_i) \\ \mathbf{0}^{3\times3} & {M_i}^{-1}\left(-C_i(\nu_i) - D_i\right) \end{bmatrix} x_i + \begin{bmatrix} \mathbf{0}^{3\times3} \\ {M_i}^{-1} \end{bmatrix} \tau_i. \end{aligned} \tag{3}$$

*1) Successively linearized model:* MPC has been popular in practical applications since its very early days [17]. For waterborne transport, MPC has been applied to control the motion of the vessels, such as, path following [7], heading control [18], and collision avoidance [19]. Besides, distributed MPC has been used for cooperative control of networked vehicles [20]. Therefore, we consider MPC as a suitable approach for the control of multiple vessels.

The dynamics described in (3) are, however, highly nonlinear. If this nonlinear model is directly used to design the MPC controller, the MPC online predictions and optimizations would be too time-consuming for real-time control. Therefore, the successively linearized model presented in [7] is adopted in this paper. The dynamic model (3) is discretized with a sample time $T_s$:

$$x_i(k+1|\,k) = x_i(k) + \int_{kT_s}^{(k+1)T_s} f_i\left(x_i(k), \tau_i(k)\right)dt. \tag{4}$$

At each time step, the controller calculates a sequence of control inputs for the whole predict horizon and only the first control sample will be implemented. In the next step, as a start point, the control sequence is shifted one sample with a extensive of zeros at the end. Using this extended control sequence as seed input $u^e\,(k|\,k)$, we can obtain the seed state $x^e(\,k+1|\,k)$ with (3). By applying Taylor's theorem and neglecting the higher order terms than the first order, we can obtain the discrete linearized model:

$$\begin{aligned} x(\,k+1|\,k) =& x^e(\,k+1|\,k) + A^{\mathrm{d}}\,(k|\,k)\,(x\,(k|\,k) - x^e\,(k|\,k)) \\ &+ B^{\mathrm{d}}\,(k|\,k)\,(u\,(k|\,k) - u^e\,(k|\,k))\,, \end{aligned} \tag{5}$$

where $A^{\mathrm{d}}$ and $B^{\mathrm{d}}$ are corresponding discrete Jacobian matrices.

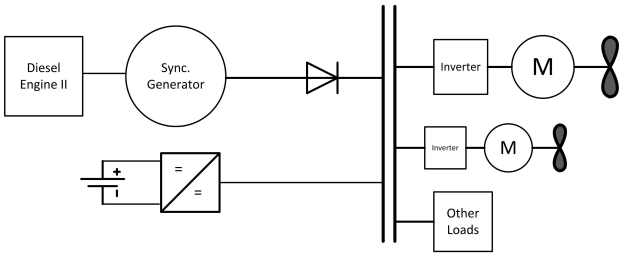


Fig. 1. A schematic view of the considered all-electric DC PPS.

### B. Power and Propulsion System

In this paper, the focus is on all-electric Power and Propulsion Systems (PPS) where the relationship between the diesel engine and propellers is established by a microgrid. A DC microgrid configuration is considered for the PPS where the generated power is distributed between energy consumers, i.e., propellers, hotel load, etc. through a DC-link. In Figure 1, a schematic view of the DC PPS is presented.

In this part, a relationship is established between the generated torque and thrust by the thrusters and the fuel efficiency which is used by the distributed MPC algorithm for Eco-VTF. The relationship between the vector of applied forces in the body-fixed frame and the generated thrust by propellers in an individual vessel is formed as:

$$\tau_i = \Gamma_{3\times m} \begin{bmatrix} T_{\mathrm{p}_1}(n_1) \\ \vdots \\ T_{\mathrm{p}_m}(n_m) \end{bmatrix}, \tag{6}$$

where $T_{\mathrm{p}_1}$, ... , $T_{\mathrm{p}_m}$ are actuators dynamics, $n_1$, ... , $n_m$ are actuators shaft speeds, $m$ is the number of actuators, and $\Gamma$ is the thrust configuration matrix defined as:

$$\Gamma = \begin{bmatrix} \gamma_1 & \ldots & \gamma_m \end{bmatrix}, \tag{7}$$

with $t_1$, $t_2$, ..., $t_m$ column vectors for standard actuators. If the actuator is a propeller, then, $\gamma_i = \begin{bmatrix} 1, 0, -l_{\mathrm{y}} \end{bmatrix}^{\mathrm{T}}$, if the actuator is a stern or bow thruster, then, $\gamma_i = \begin{bmatrix} 0, 1, l_{\mathrm{x}} \end{bmatrix}^{\mathrm{T}}$, where $l_y$ and $l_x$ are actuator positions in the ASV reference frame (Figure 2). Since, generally, $\Gamma$ is not a square matrix the solution to the problem of unconstrained thrust allocation to non-rotatable actuators can be found using the pseudo-inverse of $T$:

$$\tau_{\mathrm{ac}_i} = \Gamma^{\mathrm{T}}(\Gamma\Gamma^{-1})^{-1}\tau_{\mathrm{s}}. \tag{8}$$

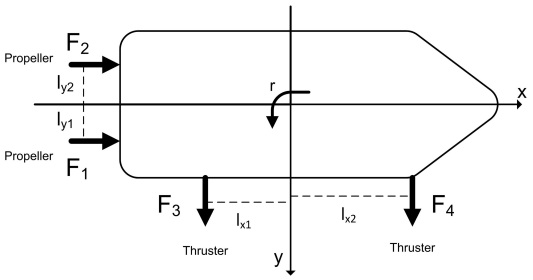


Fig. 2. An ASV with two propellers ($F_1$ and $F_2$), one stern thruster ($F_3$) and a bow thruster ($F_4$).

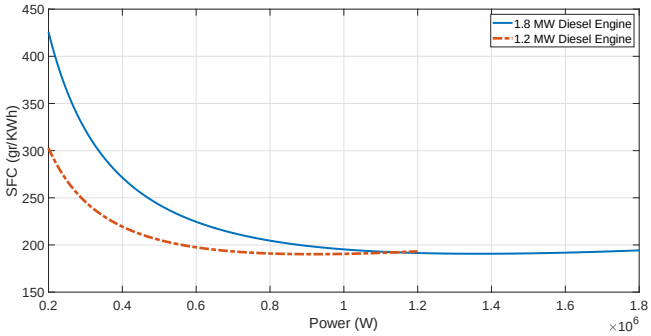


Fig. 3. SFC curve of two diesel engines with different power ratings.

The relationship between the shaft speed and propeller torque and thrust is established using the following equations [21]:

$$T_{\mathrm{p}} = K_{\mathrm{T}} \rho D^4 |n_{\mathrm{p}}| n_{\mathrm{p}} \tag{9}$$

$$Q_{\mathrm{p}} = K_{\mathrm{Q}} \rho D^5 |n_{\mathrm{p}}| n_{\mathrm{p}}, \tag{10}$$

where $D$ is the propeller diameter and $\rho$ is the water density. Parameters $K_{\mathrm{T}}$ and $K_{\mathrm{Q}}$ are thrust and torque coefficients which are functions of propeller structure and advance ratio. Using the above equations the produced power a propeller can be calculated as:

$$P_{\mathrm{p}} = 2\pi Q_{\mathrm{p}} n_{\mathrm{p}} = 2\pi K_{\mathrm{Q}} \rho D^5 n_{\mathrm{p}}^3. \tag{11}$$

Using the efficiency curve of the induction motors, the overall absorbed power by the propulsive loads can be estimated [1]. This efficiency is normally between 70% to 95% depending on the loading condition. In the context of this paper, a constant coefficient is chosen to represent the efficiency of the induction motor since for lading conditions above 20% of full load, the efficiency converges to a constant number [2]. As a result, the overall load power at the DC-link for vessel $i$ is:

$$P_{\mathrm{d}_i} = \frac{P_{\mathrm{p}_1}}{\alpha_{\mathrm{p}_1}} + \frac{P_{\mathrm{p}_2}}{\alpha_{\mathrm{p}_2}} + ... + \frac{P_{\mathrm{p}_\mathrm{m}}}{\alpha_{\mathrm{p}_\mathrm{m}}} \tag{12}$$

where $\alpha_{\mathrm{p}_1}$, ..., $\alpha_{\mathrm{p}_\mathrm{m}}$ are efficiency coefficients of the on-board induction motors.

The fuel efficiency of a diesel engine with regard to the produced power is presented using the Specific Fuel Consumption (SFC) curve of the engine that is: The SFC curve function of a diesel engine can be shown by the below equation:

$$SFC(P_{\mathrm{en}}) = \frac{a}{P_{\mathrm{en}}} + bP_{\mathrm{en}} + c \tag{13}$$

where $P_{\mathrm{en}}$ is the delivered mechanical power and $a$, $b$ and $c$ are parameters dependent on the diesel engine specifications. The SFC curves of two diesel engines that are used in this paper are shown in Figure 3. The figure indicates that under low power loading the diesel engine is inefficient while as the load increases the efficiency increases and in high loading conditions it decreases. During low power demand periods, the battery can be used although it is not a concrete solution for the efficiency issue due to limited capacity and relatively lower power delivery compared to diesel engines.

The electrical losses in energy generation side of the power network are included in the problem by a constant coefficient, i.e., $P_{\mathrm{DGR}} = \alpha_{\mathrm{DGR}} P_{\mathrm{en}}$ where $0 < \alpha_{\mathrm{DGR}} < 1$ and depends on the specifications of the generator-rectifier set. $P_{\mathrm{DGR}}$ is the generated power by the diesel-generator-rectifier set. The same approach is also considered for the set of battery-converter. As a result, $P_{\mathrm{BC}} = \alpha_{\mathrm{BC}} P_{\mathrm{B}}$ where $0 < \alpha_{\mathrm{BC}} < 1$. Since, the efficient region in the SFC curve is a wide area, this approximation does not affect the optimality of the process, significantly. Then, for power availability in vessel $i$,

$$P_{\mathrm{d}_i} = \alpha_{\mathrm{BC}_i} P_{\mathrm{B}_i} + \alpha_{\mathrm{DGR}_i} P_{\mathrm{en}_i}. \tag{14}$$

The objective in this paper is to guarantee the maximal fuel efficiency for the platoon by maximizing the efficiency in individual vessels. This maximum efficiency obtained through negotiations between vessel and eventually a consensus on the platoon speed. In the next section, a distributed control algorithm is presented to guarantee efficiency in VTFs.

## III. Vessel Train Formation

### A. Formulation of the VTF problem based on speed consensus

Vessels usually have predetermined origins, destinations and paths. To sailing in groups, the speed of the vessels becomes consensus. At the same time, vessels should avoid collision with nearby vessels. Thus, in the VTF problem, the following three rules are applied:

- Trajectory following: attempt to follow the predetermined paths;
- Speed consensus: attempt to keep the same speed with nearby vessels;
- Collision avoidance: avoid collisions with nearby vessels.

According to the three rules, the objective of a single vessel in a vessel train can be described as

$$\begin{aligned} J_i\left(\tau_i(k)\right) = \sum_{l=1}^{H_{\mathrm{p}}} \sum_{j \in N_i} & \left(\alpha \| \eta_i(k+l\,|k) - w_i(k+l) \|_2 \right. \\ & + \beta \| \eta_i(k+l\,|k) - \vartheta_{N_i}(k+l\,|k) \|_2 \\ & \left. + \gamma \| \tau_i(k+l-1\,|k) \|_2 \right). \end{aligned} \tag{15}$$

The three parts in the equation represent trajectory following, speed consensus and control efforts, respectively: $\alpha$, $\beta$ and $\gamma$ are the weights; $N_i$ is the set of neighbors of vessel $i$, $N_i = \{j \in \mathcal{V} : \|p_j - p_i\|_2 \leqslant \Upsilon_i\}$, $p_i$ is the position of vessel $i$, $p_i = [x_i, y_i]^{\mathrm{T}}$; $H_{\mathrm{p}}$ is the prediction horizon; $l$ is the $l$th time step in the prediction horizon; $\eta_i(k+l\,|k)$ is the prediction made at $k$ about the position and heading of vessel $i$ at $k+l$; $w_i(k+l)$ is the reference at $k+l$, including trajectory and heading; $\vartheta_{N_i}(k+l\,|k) = [\bar{p}_i(k+l\,|k), \bar{\psi}_i(k+l\,|k)]$ is the speed consensus state (position $\bar{p}_i(k+l\,|k)$ and heading $\bar{\psi}_i(k+l\,|k)$) at $k+l$ calculated according to the average speed of neighbors of vessel $i$ at $k$. The speed consensus position $\bar{p}_i$ is calculated with a double integrator dynamics, $\bar{p}_i(k+l\,|k) = p_i(k) + l\bar{v}_i(k)$. $\bar{v}_i(k)$ is the consensus velocity, with a magnitude equals to the desired consensus speed and direction to new waypoint, $\|\bar{v}_i(k)\|_2 = \frac{\left(\hat{v}_i(k) + \sum_{l=1}^{H_{\mathrm{p}}} \sum_{j \in N_i} \left\|[u_j(k+l|k), v_j(k+l|k)]^{\mathrm{T}}\right\|_2\right)}{N_{N_i}+1}$, $\hat{v}_i(k)$ is the planned speed of $i$, $N_{N_i}$ is the number of neighbors. The speed consensus heading is determined according to $\bar{p}_i$, and the changes between heading should be within the range[-$\pi$, $\pi$]; $\tau_i(k)$ indicates control input over the prediction horizon.

Therefore, the optimization problem that each ASV in a vessel train needs to solve is as follows:

Problem $\mathscr{A}$:

$$\begin{aligned}
\min \quad & J_i\left(\tau_i(k)\right) \\
\text{s.t.} \quad & \forall i \in \mathcal{V}, \forall j \in N_i, \forall l \in H_{\mathrm{p}}: \\
& \nu_{i,\min} \leqslant \nu_i(k+l\,|k) \leqslant \nu_{i,\max} && (16)\\
& \tau_{i,\min} \leqslant \tau_i(k+l\,|k) \leqslant \tau_{i,\max} && (17)\\
& d_{ij|i}\,(k+l\,|k) \geqslant d_{\mathrm{ij,safe}} && (18)\\
& p_i \in \Xi && (19)\\
& \text{Dynamics described by (5),}
\end{aligned}$$

where $\nu_{i,\min}$, $\nu_{i,\max}$ and $\tau_{i,\min}$, $\tau_{i,\max}$ are the constraints on states and control inputs; $d_{ij|i}(k+l\,|k) = \left\|p_i(k+l\,|k) - p_{j|i}\,(k+l\,|k)\right\|_\infty$; $p_{j|i}$ is the position of $j$ that $i$ received; $d_{\mathrm{ij,safe}}$ is safety distance between vessel $i$ and $j$; $\Xi$ indicates navigable waters.

In this cooperation problem, each vessel controller (VC) makes decisions based on the information provided by other controllers. Therefore, an agreement is achieved when the actions each controller want to take reach a consensus with the information it broadcasts.

The interconnecting variables that link the control problems of different vessels are the predicted trajectories of the ASVs. Thus the information being exchanged, $ZX_a^s$ consists of the predicted trajectories determined with the control inputs the vessels calculated in each iteration and the nonlinear dynamic model (3).

The Alternating Direction Method of Multipliers (ADMM) is one of the widely applied methods to solve consensus problems iteratively [22]. The algorithm firstly forms the augmented Lagrangian of Problem $\mathscr{A}$. Then, the primal variables and the dual variable are updated to make the control variables and the broadcast variables converge. To sum up, the VTF control of vessels in a vessel train $\mathcal{VT}_\iota$ consists of the following steps at each time step $k$:

Step 1: VC $i \in \mathcal{VT}_\iota$ determines the control input $\tau_i^s(k)$ by solving the Augmented Lagrange form of Problem $\mathscr{A}$ with $p_{j|i}^s = \left[\mathbf{I}^{2\times 2} \quad \mathbf{0}^{2\times 4}\right] ZX_i^s(k)$:

$$\begin{aligned}
\tau_i^s(k) = & \underset{\tau_i(k)}{\arg\min} \left(J_i\left(\tau_i(k)\right)\right. \\
& + \left(\lambda_i^{s-1}\right)^T \left(\tau_i(k) - z_i^{s-1}(k)\right) \\
& \left. + \rho_i/2 \ \left\|\tau_i(k) - z_i^{s-1}(k)\right\|_2^2\right).
\end{aligned}$$

If solution do not exist, $\tau_i^s(k) = \tau_i^{s-1}(k)$

Step 2: VC $i$ updates the global variable $z_i^s(k)$, Lagrange multipliers $\lambda_i^s(k)$, primal residual $R_{\mathrm{pri},i}^s$ and dual residual $R_{\mathrm{dual},i}^s$:
$z_i^s := \varphi_i \tau_i^s + (1-\varphi_i)\, z_i^{s-1} + \lambda_i^{s-1}/\rho_i$;
$\lambda_i^s := \lambda_i^{s-1} + \rho_i\left(\tau_i - z_i^s\right)$;
$R_{\mathrm{pri},i}^s := \tau_i^s - z_i^s$;
$R_{\mathrm{dual},i}^s := z_i^s - z_i^{s-1}$;
$\varepsilon_{\mathrm{pri},i}^s := \sqrt{Nn_u}\varepsilon^{\mathrm{abs}} + \varepsilon^{\mathrm{rel}} \max\left\{\|u_i^s\|_2, \|z_i^s\|_2\right\}$;
$\varepsilon_{\mathrm{dual},i}^s := \sqrt{Nn_u}\varepsilon^{\mathrm{abs}} + \varepsilon^{\mathrm{rel}}\|\lambda_i^s\|_2$;

Step 3: VC $i$ updates interconnecting variable $ZX_i^s(k)$ according to (3), and send it to other VCs;

Step 4: The next VC $j$ repeats Step 1-3 until all the VCs finish computation;

Step 5: Each VC moves on to the next iteration $s+1$ and repeat Step 1-4 until the following stopping criteria is met $\forall i \in \mathcal{VT}_\iota$:

$$\left\|R_{\mathrm{pri},i}^s\right\|_2 \leqslant \varepsilon_{pri,i}^s \text{ and } \left\|R_{\mathrm{dual},i}^s\right\|_2 \leqslant \varepsilon_{\mathrm{dual},i}^s, \quad (20)$$

The sequence of VCs to carry out computation can be different, such as in order, in reverse, iterative or random. Details about the VTF problem are addressed in [15].

### *B. Eco-VTF*

In a vessel train, there can be several vessels with different specifications that ranged from vessel size and shape to power ratings. As a result, their suitable operating profiles might differ. One of the primary objectives in this paper is to enable fuel efficient VTF that is maneuvering of autonomous ships in a train formation with the most efficient speed for the overall vessels. Therefore, the proposed approach, Eco-VTF, leads to a consensus on a speed for the platoon that is optimal for all the vessels subject to their operational objectives and efficiency specification of their PPS.

According to Section II-B, power is a function of the control force and moment:

$$P_i(k) = h(x(k), \tau_i(k)). \quad (21)$$

To guarantee the fuel efficiency, the power should be within the efficient region in the SFC curve. Therefore, in the Eco-VTF problem, the optimization problem that each

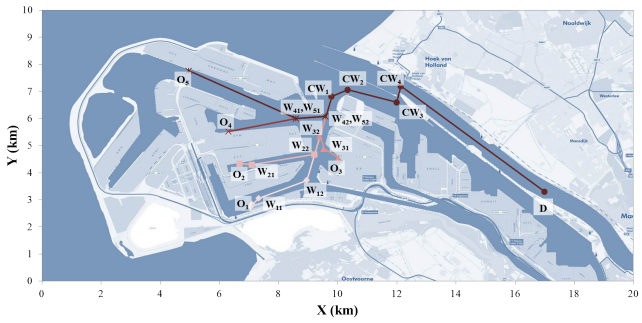


Fig. 4. Simulation area and waypoints.

TABLE I
WAYPOINTS OF EACH ASV

| | ASV 1 | | ASV 2 | | ASV 2 | | ASV 4 | | ASV 5 | |
|---|---|---|---|---|---|---|---|---|---|---|
| (km) | X | Y | X | Y | X | Y | X | Y | X | Y |
| $O_i$ | 7.12 | 2.84 | 6.7 | 4.34 | 10.04 | 4.54 | 6.32 | 5.52 | 4.98 | 7.76 |
| $W_{i1}$ | 7.34 | 3.06 | 7.1 | 4.3 | 9.54 | 4.88 | 8.6 | 6 | 8.6 | 6 |
| $W_{i2}$ | 8.96 | 3.72 | 9.22 | 4.68 | 9.4 | 5.34 | 9.6 | 6.08 | 9.6 | 6.08 |
| $CW_1$ | 9.8 | 6.82 | 9.8 | 6.82 | 9.8 | 6.82 | 9.8 | 6.82 | 9.8 | 6.82 |
| $CW_2$ | 10.34 | 7.06 | 10.34 | 7.06 | 10.34 | 7.06 | 10.34 | 7.06 | 10.34 | 7.06 |
| $CW_3$ | 12 | 6.6 | 12 | 6.6 | 12 | 6.6 | 12 | 6.6 | 12 | 6.6 |
| $CW_4$ | 12.14 | 7.2 | 12.14 | 7.2 | 12.14 | 7.2 | 12.14 | 7.2 | 12.14 | 7.2 |
| $D_i$ | 17 | 3.3 | 17 | 3.2 | 17 | 3.2 | 17 | 3.2 | 17 | 3.2 |

vessel needs to solve (in Step 1) is:

$$\begin{aligned}\min \quad J_i\left(\tau_i(k)\right) = \sum_{l=1}^{H_\mathrm{p}} \sum_{j\in N_i} & \left(\alpha\|\eta_i(k+l\,|k) - w_i(k+l)\|_2\right. \\ & +\beta\|\eta_i(k+l\,|k) - \vartheta_{N_i}(k+l\,|k)\|_2 \\ & \left.+\gamma\|\,|\tau_i(k+l-1\,|k)| - \delta_i(k+l-1\,|k)\|_2\right), \end{aligned} \tag{22}$$

$$\text{s.t.} \quad \tau_{i,low}^{eff} \leqslant \delta_i(k+l-1\,|k) \leqslant \tau_{i,up}^{eff},\ \forall l \in H_\mathrm{p}, \tag{23}$$

constraints in Problem $\mathscr{A}$.

## IV. SIMULATION EXPERIMENTS

In this section, a simulation of a vessel train consisting of 5 vessels navigating from the different terminals in the Port of Rotterdam to inland waterways is presented. The experiments are carried out with Matlab 2016a. The optimization problems of the controllers are solved by ILOG CPLEX Optimization Studio (Version 12.6.3). The experiments are run on a PC with a dual-core 3.2GHz Intel(R) Core(TM) i5-3470U CPU and 8GB of RAM.

### A. Set up

The simulation area is shown in Figure 4. Five ASVs start from different terminal $(O_1, \ldots, O_5)$, and they navigate together through the inland waterways. The vessels have reference paths indicated by waypoints. The position of the origins, waypoints and the destination are listed in Table I. Vessels start to form the vessel train when they arrive at $W_{i2}$. The start time of each ASV is different, ASV 1-5 set off in time step 1, 35, 180, 1, 95, respectively.

TABLE II
ASVS IN SIMULATION

| | | ASV 1 | ASV 2 | ASV 3 | ASV 4 | ASV 5 |
|---|---|---|---|---|---|---|
| Dynamic model[a] | | I | II | I | II | I |
| Planned | Model | 0.6 | 0.5 | 0.3 | 0.4 | 0.7 |
| Speed (m/s) | Reality | 3.2863 | 2.7386 | 1.6432 | 2.1909 | 3.8341 |
| $d_{i,\mathrm{safe}}$ (m)[b] | Model | 0.25 | 0.6 | 0.25 | 0.6 | 0.25 |
| | Reality | 1.3693 | 3.2863 | 1.3693 | 3.2863 | 1.3693 |
| Max power | DC | 2040 | 1200 | 1800 | 1760 | 2720 |
| (kw) | Battery | | | 20% DC | | |
| Efficiency | Lower | 50% | 70% | 75% | 70% | 50% |
| Power | Upper | 85% | 90% | 95% | 90% | 85% |
| Efficiency | Lower | 0.6751 | 1.0792 | 0.7613 | 1.3932 | 0.8178 |
| Force (N) | Upper | 0.8846 | 1.2337 | 0.8647 | 1.5926 | 1.0717 |

[a] I: Delfia 1*; II: CyberShip;
[b] When two ASVs encountered, the safety distance between ASV $i$ and ASV $j$ is $d_{ij,safe} = (d_{i,safe} + d_{j,safe})/2$.

The five ASVs have different dynamics and engine settings. Two model vessels are used in the simulation experiments, Delfia 1* and CyberShip 2. Delfia 1* is an ASV prototype developed by TU Delft. Its shape is designed to make maneuvering applications in crowded environments easier than actual solutions allowing at the same time the possibility to cooperate with multiple ASVs. CyberShip 2 is a scale replica of a supply ship [23]. To simplified the model, we assume that each ASV has a propeller at the bow which provide surge force, and a bow thruster which provides yaw moment. The models are scaled-up according to Froude scaling law with a scaling factor $1:30$. According to the scaling law, the multiplication factors for length, force, moment and time are 30, $30^3$, $30^4$, and $\sqrt{30}$, respectively. Detail settings of each ASV are shown in Table II. The limitations of velocity and force/moment for the 5 ASVs are $\tau_{\max} = [2, 0, 1.5]^\mathrm{T}$, $\tau_{\max} = -\tau_{\max}$, $\nu_{\max} = [0.7, 0.7, 20\pi/180]^\mathrm{T}$, $\nu_{\min} = [0, -0.7, -20\pi/180]^\mathrm{T}$.

Each ASV is controlled by an MPC controller, with $\alpha = \begin{bmatrix} 5 & 0 & 0 \\ 0 & 5 & 0 \\ 0 & 0 & 50 \end{bmatrix}$, $\beta = 2\alpha$, $\gamma = 2$, $H_\mathrm{p} = 10$, and $\varepsilon^{\mathrm{abs}} = \varepsilon^{\mathrm{rel}} = 10^{-3}$.

### B. Simulation results

Fig. 5-8 show the results of simulations using VTF and Eco-VTF algorithms. Fig. 5 shows the trajectories of ASVs. Vessels have the similar trajectories in the experiments using Eco-VTF and VTF. Fig. 6 provides the linear and angular velocities and forces and moments of the ASVs in the simulation. Due to the speed consensus rule, the velocities of the ASVs become similar using both VTF and Eco-VTF. As each ASVs have its own preferred planned speed, there are differences in speed among the ASVs. In the experiment using VTF algorithm, the consensus speed is higher than the speed when ASVs using Eco-VTF. Moreover, vessels using VTF changes their velocity more frequently, which also lead to higher fuel consumption rate (Fig. 7) and total fuel consumption (Fig. 8). ASVs using Eco-VTF have lower

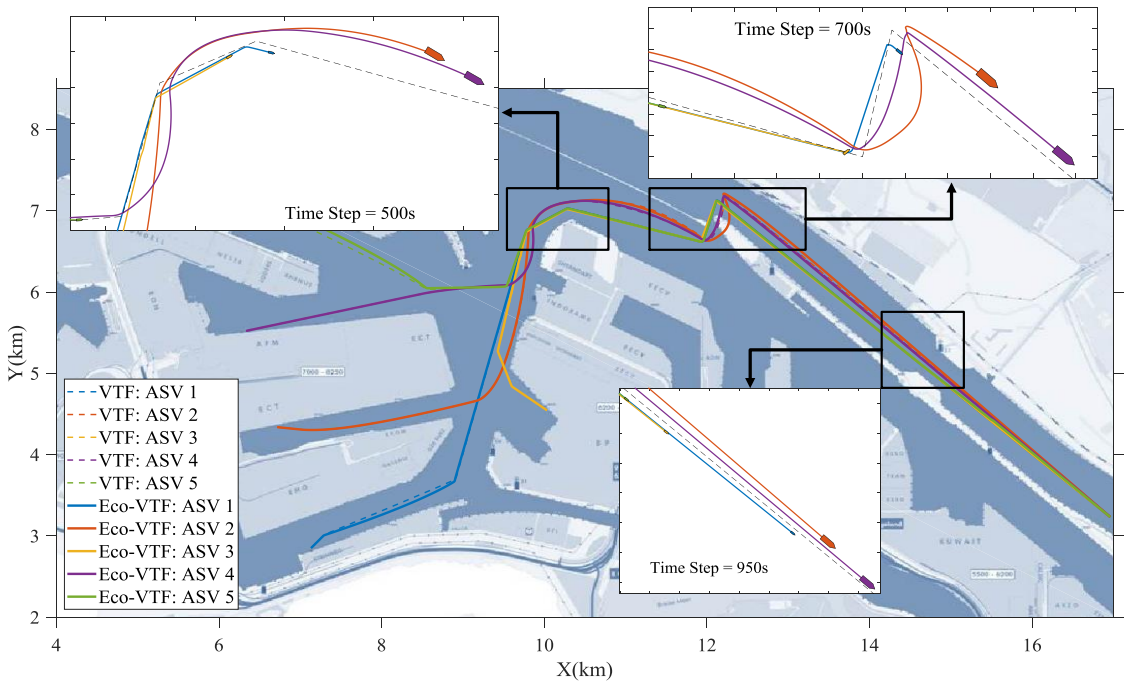


Fig. 5. Trajectories of the ASVs in simulation using Eco-VTF.

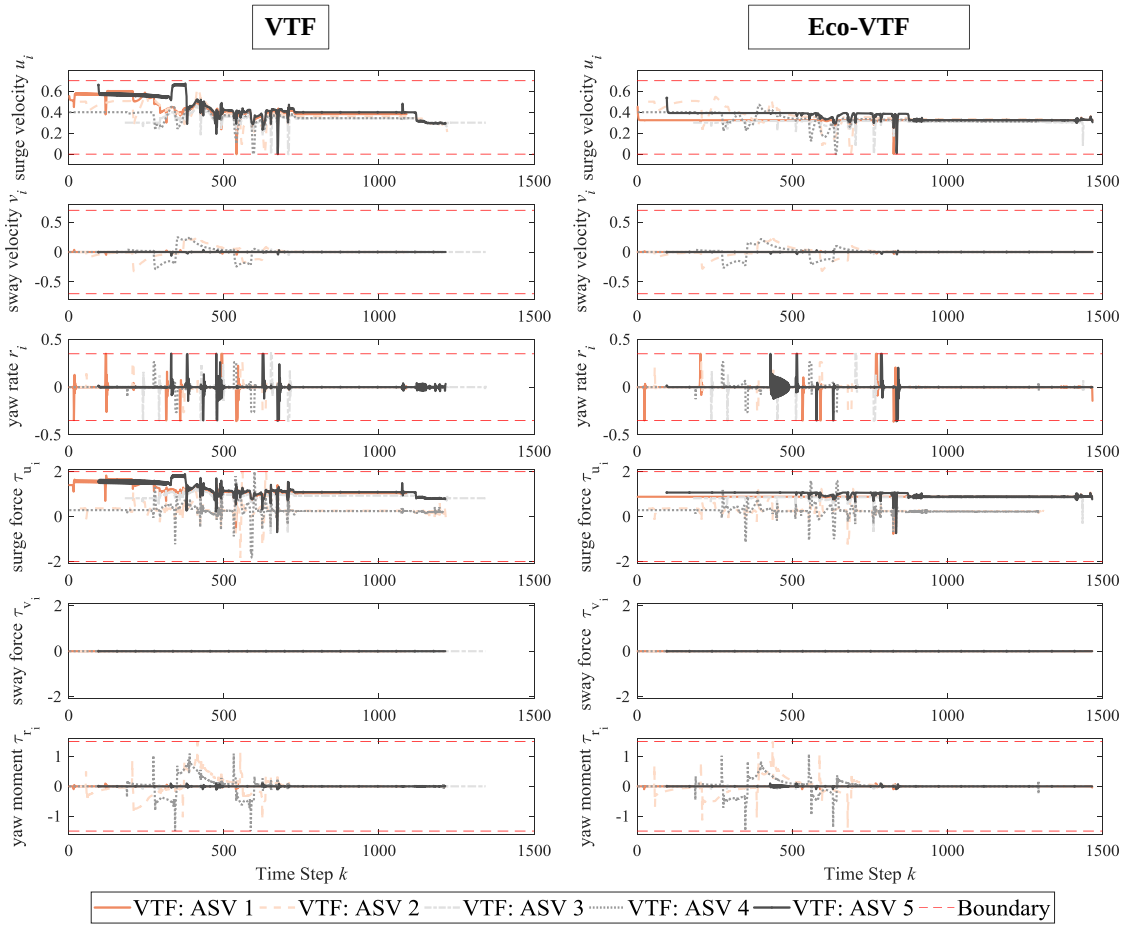


Fig. 6. Comparison of $\nu$ and $\tau$ of ASVs using VTF and Eco-VTF.

TABLE III

COMPARISON OF THE SIMULATION RESULTS

| | | ASV 1 | ASV 2 | ASV 3 | ASV 4 | ASV 5 |
|---|---|---|---|---|---|---|
| VTF | Average Speed (m/s) | 0.44 | 0.39 | 0.33 | 0.37 | 0.44 |
| | Average FCR (g/s) | 163.53 | 14.12 | 89.61 | 16.91 | 143.68 |
| | Fuel $\times 10^5$(g) | 9.74 | 0.94 | 6.59 | 1.12 | 9.55 |
| Eco-VTF | Average Speed (m/s) | 0.32 | 0.37 | 0.30 | 0.34 | 0.36 |
| | Average FCR (g/s) | 92.17 | 11.48 | 75.40 | 15.15 | 98.25 |
| | Fuel $\times 10^5$(g) | 7.41 | 0.82 | 5.95 | 1.07 | 7.89 |
| Difference[a] | Average Speed (m/s) | -0.11 | -0.02 | -0.03 | -0.02 | -0.08 |
| | Average FCR (g/s) | -71.36 | -2.63 | -14.22 | -1.76 | -45.44 |
| | Fuel $\times 10^5$(g) | -2.34 | -0.12 | -0.65 | -0.05 | -1.66 |
| FCR improvement | | -43.6% | -18.7% | -15.9% | -10.4% | -31.6% |
| Fuel improvement | | -24.0% | -12.5% | -9.8% | -4.2% | -17.4% |

[a] Difference=Eco-VTF – VTF; [b] Improvement=Difference/VTF.

speed, and thus, longer total travel time. However, Eco-VTF helps a lot in reducing the fuel consumption. Table III provides the comparison of average speed, average FCR and total fuel consumption of the experiments using VTF and Eco-VTF. A significant amount of fuel saving can be obtained by using Eco-VTF, especially for the ASVs with higher maximum engine power, such as ASV 1 and ASV 5.

## V. CONCLUSIONS AND FUTURE RESEARCH

In this paper, the problem of enabling fuel efficient vessel train formation has been investigated where a distributed control approach is presented for path following, collision avoidance and speed consensus among the vessels. Simulation experiments are carried out in the port of Rotterdam waterways with replica model DC electric autonomous vessels. The results suggest that by adopting the proposed Eco-VTF approach, a significant amount of efficiency and reduced emissions can be obtained.

The future research in this framework consists of extending the results to the whole port to study the amount of fuel saving and emission reduction if a considerable share of voyages in the port area are carried out using the proposed strategy.

## ACKNOWLEDGMENT

This research is supported by the China Scholarship Council under Grant 201406950041 and the project ShipDrive: A Novel Methodology for Integrated Modelling, Control, and Optimization of Hybrid Ship Systems (project 13276) of the Netherlands Organisation for Scientific Research (NWO), domain Applied and Engineering Sciences (TTW).

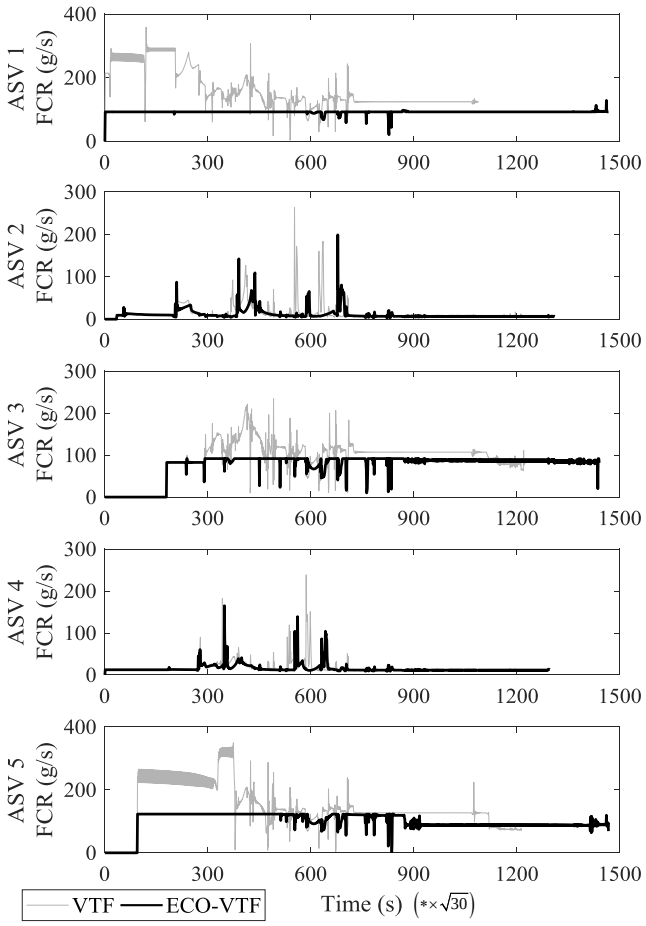


Fig. 7. Fuel consumption rate of each ASV.

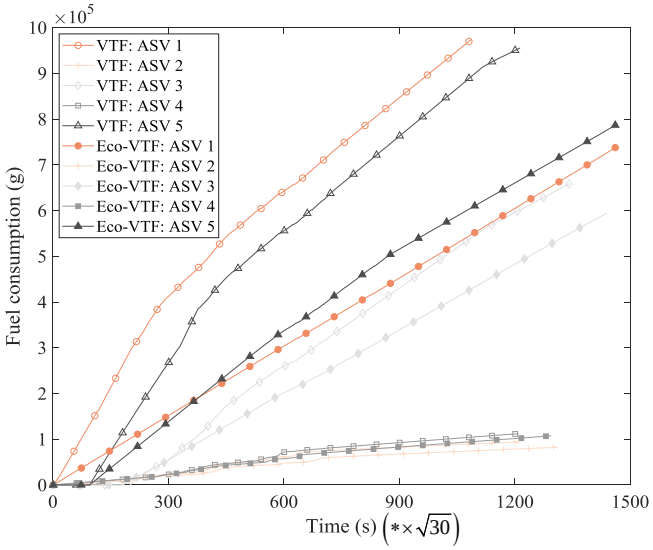


Fig. 8. Total fuel consumption of each ASV.

## APPENDIX

## PARAMETERS OF THE REPLICA MODEL VESSELS

The maneuvering model parameters of the two model vessels are provided in Table IV.

TABLE IV

PARAMETERS FOR DELFIA 1* AND CYBERSHIP 2[a]

| Parameter | Delfia 1* | CyberShip 2[b] |
|---|---|---|
| $m$ | 3.345 | 23.80 |
| $I_z$ | 0.031 | 1.760 |
| $x_g$ | 0.0 | 0.046 |
| $X_u$ | -2.734 | -0.7225 |
| $Y_v$ | -4.60250 | -0.8612 |
| $Y_r$ | 0.79546 | -0.1079 |
| $N_v$ | 0.50439 | 0.1052 |
| $N_r$ | -0.22243 | -1.900 |
| $X_{\dot{u}}$ | -0.2310 | -2.0 |
| $Y_{\dot{v}}$ | -1.334 | -10.0 |
| $Y_{\dot{r}}$ | 0.0 | 0.0 |
| $N_{\dot{r}}$ | -0.110 | -1.0 |

[a] The hydrodynamic derivatives follow the notations in [24];
[b] Data about CyberShip 2 are from [23].

## PARAMETERS OF THE SFC CURVES

I. 1.2 MW diesel engine: $a = 3.68 \times 10^7\ gr.KWh$, $b = 4.40 \times 10^{-5}\ gr/KWh^2$, $c = 109.60\ gr/KWh$.
II. 1.8 MW diesel engine: $a = 6.45 \times 10^7\ gr.KWh$, $b = 3.45 \times 10^{-5}\ gr/KWh^2$, $c = 96.21\ gr/KWh$.
III. 2.72 MW diesel engine: $a = 6.23 \times 10^7\ gr.KWh$, $b = 7.58 \times 10^{-6}\ gr/KWh^2$, $c = 147.1\ gr/KWh$.
IV. 2.04 MW diesel engine: $a = 4.67 \times 10^7\ gr.KWh$, $b = 1.01 \times 10^{-5}\ gr/KWh^2$, $c = 147.1\ gr/KWh$.
V. 1.76 MW diesel engine: $a = 6.30 \times 10^7\ gr.KWh$, $b = 3.42 \times 10^{-5}\ gr/KWh^2$, $c = 98.23\ gr/KWh$.

## REFERENCES


[1] A. Haseltalab and R. R. Negenborn, "Predictive on-board power management for all-electric ships with DC distribution architecture," in *Proceedings of the OCEANS 2017 MTS/IEEE Aberdeen*, June 2017, pp. 1–8.

[2] R. D. Geertsma, R. R. Negenborn, K. Visser, and J. J. Hopman, "Design and control of hybrid power and propulsion systems for smart ships: A review of developments," *Applied Energy*, vol. 194, pp. 30 – 54, 2017. [Online]. Available: http://www.sciencedirect.com/science/article/pii/S0306261917301940

[3] C. A. Thieme, I. B. Utne, and S. Haugen, "Assessing ship risk model applicability to marine autonomous surface ships," *Ocean Engineering*, vol. 165, pp. 140 – 154, 2018. [Online]. Available: http://www.sciencedirect.com/science/article/pii/S0029801818313210

[4] S. L. Dai, M. Wang, and C. Wang, "Neural learning control of marine surface vessels with guaranteed transient tracking performance," *IEEE Transactions on Industrial Electronics*, vol. 63, no. 3, pp. 1717–1727, March 2016.

[5] J. Velagic, Z. Vukic, and E. Omerdic, "Adaptive fuzzy ship autopilot for track-keeping," *Control Engineering Practice*, vol. 11, no. 4, pp. 433 – 443, 2003, mCMC00. [Online]. Available: http://www.sciencedirect.com/science/article/pii/S0967066102000096

[6] A. Haseltalab and R. R. Negenborn, "Adaptive control for a class of partially unknown non-affine systems: Applied to autonomous surface vessels," *IFAC-PapersOnLine*, vol. 50, no. 1, pp. 4252 – 4257, 2017, 20th IFAC World Congress. [Online]. Available: http://www.sciencedirect.com/science/article/pii/S2405896317312879

[7] H. Zheng, R. R. Negenborn, and G. Lodewijks, "Predictive path following with arrival time awareness for waterborne AGVs," *Transportation Research Part C: Emerging Technologies*, vol. 70, pp. 214–237, 2016.

[8] H. Zheng, "Coordination of waterborne AGVs," Ph.D. dissertation, Delft University of Technology, 2016.

[9] I. Georgescu, M. Godjevac, and K. Visser, "Efficiency constraints of energy storage for on-board power systems," *Ocean Engineering*, vol. 162, pp. 239 – 247, 2018. [Online]. Available: http://www.sciencedirect.com/science/article/pii/S0029801818307030

[10] M. Kalikatzarakis, R. D. Geertsma, E. J. Boonen, K. Visser, and R. R. Negenborn, "Ship energy management for hybrid propulsion and power supply with shore charging," *Control Engineering Practice*, vol. 76, pp. 133 – 154, 2018. [Online]. Available: http://www.sciencedirect.com/science/article/pii/S096706611830090X

[11] A. S. Jain and S. Meeran, "A state-of-the-art review of job-shop scheduling techniques," Technical report, Department of Applied Physics, Electronic and Mechanical Engineering, University of Dundee, Dundee, Scotland, Tech. Rep., 1998.

[12] B. Zahedi and L. Norum, "Modeling and simulation of all-electric ships with low-voltage dc hybrid power systems," *IEEE Transactions on Power Electronics*, vol. 28, no. 10, pp. 4525–4537, Oct 2013.

[13] H. Zheng, R. R. Negenborn, and G. Lodewijks, "Fast ADMM for distributed model predictive control of cooperative waterborne AGVs," *IEEE Transactions on Control Systems Technology*, vol. 25, no. 4, pp. 1406–1413, 2017.

[14] ——, "Robust distributed predictive control of waterborne AGVs –a cooperative and cost-effective approach," *IEEE Transactions on Cybernetics*, vol. 48, no. 8, pp. 2449–2461, 2018.

[15] L. Chen, H. Hopman, and R. R. Negenborn, "Distributed model predictive control for vessel train formations of cooperative multi-vessel systems," *Transportation Research Part C: Emerging Technologies*, vol. 92, pp. 101–118, 2018.

[16] T. I. Fossen, *Handbook of marine craft hydrodynamics and motion control*. United Kingdom: John Wiley & Sons Ltd, 2011.

[17] R. R. Negenborn and J. M. Maestre, "Distributed model predictive control: an overview and roadmap of future research opportunities," *IEEE Control Systems Magazine*, vol. 34, no. 4, pp. 87–97, 2014.

[18] Z. Li and J. Sun, "Disturbance compensating model predictive control with application to ship heading control," *IEEE Transactions on Control Systems Technology*, vol. 20, no. 1, pp. 257–265, 2012.

[19] M. Abdelaal, M. Fräzle, and A. Hahn, "NMPC-based trajectory tracking and collison avoidance of underactuated vessels with elliptical ship domain," *IFAC-PapersOnLine*, vol. 49, no. 23, pp. 22–27, 2016.

[20] T. Keviczky, F. Borrelli, K. Fregene, D. Godbole, and G. J. Balas, "Decentralized receding horizon control and coordination of autonomous vehicle formations," *IEEE Transactions on Control Systems Technology*, vol. 16, no. 1, pp. 19–33, 2008.

[21] R. Izadi-Zamanabadi and M. Blanke, "A ship propulsion system as a benchmark for fault-tolerant control," *Control Engineering Practice*, vol. 7, no. 2, pp. 227 – 239, 1999. [Online]. Available: http://www.sciencedirect.com/science/article/pii/S096706619800149X

[22] S. Boyd, N. Parikh, E. Chu, B. Peleato, and J. Eckstein, "Distributed optimization and statistical learning via the alternating direction method of multipliers," *Foundations and Trends in Machine Learning*, vol. 3, no. 1, pp. 1–122, 2011.

[23] R. Skjetne, T. I. Fossen, and P. V. Kokotović, "Adaptive maneuvering, with experiments, for a model ship in a marine control laboratory," *Automatica*, vol. 41, no. 2, pp. 289–298, 2005.

[24] SNAME, "Nomenclature for treating the motion of a submerged body through a fluid," The Society of Naval Architects and Marine Engineers, Tech. Rep., 1952.